Numerical Determination of the Efficiency of Entrainment in Volcanic Eruption Columns

Project Representative
Takehiro Koyaguchi Earthquake Research Institute, University of Tokyo

Authors
Yujiro Suzuki Institute for Research on Earth Evolution, Japan Agency for Marine-Earth Science and Technology
Takehiro Koyaguchi Earthquake Research Institute, University of Tokyo

Entrainment of air by turbulent mixing plays a central role in the dynamics of eruption clouds; the amount of entrained air controls eruption styles and heights of eruption columns. The efficiency of entrainment is quantified by the entrainment coefficient: the ratio between mean inward radial velocity at the edge and the mean vertical velocity. We directly determined the entrainment coefficient of eruption columns as a function of height on the basis of three-dimensional numerical simulations. The value of entrainment coefficient is similar to that for pure jets (~0.07) just above the vent, and approaches that for pure plumes (0.10 – 0.15) far from the vent. Between these two regions, we identify a new transitional zone with a significantly small entrainment coefficient (~0.05). This spatial variation in the entrainment coefficient is correlated with the change in vortical structure just above the vent.

Keywords: volcanic eruption cloud, pseudo-gas model, turbulent mixing, volcanic hazard

1. Introduction

During explosive eruptions, a mixture of volcanic gas and pyroclasts is released from a vent with a density larger than the atmospheric density. As the ejected material entrains ambient air through turbulent mixing, the density of the eruption clouds decreases because the entrained air expands by heating from the hot pyroclasts. Since the density of the mixture of the ejected material plus the entrained air changes with their mixing ratio, the efficiency of entrainment controls the dynamics and heights of eruption clouds [1-5]. If the amount of entrained air is sufficient, an eruption column convectively rises, whereas, if it is insufficient, a heavy pyroclastic flow spreads on the ground surface.

The flow of an eruption cloud is modeled as a free boundary shear flow. Here, we refer to turbulent free boundary shear flows driven by initial momentum as pure jets and those driven by buoyancy as pure plumes. When a pure jet or plume is ejected from a point source into a uniform environment, the flow is characterized by the self-similarity. Turbulent mixing in and around a strictly self-similar flow can be explained by the entrainment hypothesis that the entrainment velocity at the edge of a turbulent jet and/or plume, U_e, is proportional to the mean vertical velocity, W, at each height as $U_e=kW$ [1]. The proportionality constant, k, represents the efficiency of entrainment and is called the entrainment coefficient. Experimental studies suggest that pure jets and plumes are approximated by self-similar flows with constant k (~0.07 for jets and 0.10 – 0.15 for plumes) [6, 7] .

Unlike pure jets or plumes, the flow of an eruption cloud is not self-similar. Its driving force changes with height because of the change in density. The flow near the vent has negative buoyancy and is driven by the initial momentum. As the eruption column rises, the density of the cloud decreases and the flow is primarily driven by positive buoyancy. Recent theoretical studies have suggested that the entrainment coefficient of such a non-self-similar flow is not necessarily constant [3]; however, no previous studies have succeeded in determining how the entrainment coefficient spatially varies in eruption clouds. The lack of knowledge of the spatial variation of entrainment coefficient has been a fundamental obstacle for understanding the entrainment mechanisms. In this study, we determine the value of k as a function of height (referred to as `local k´) using three -dimensional (3-D) simulations of an eruption column.

2. Model for Determining k by 3-D Model

The simulations are based on a 3-D time-dependent fluid dynamics model that solves a set of partial differential equations describing the conservation of mass, momentum, and energy, and constitutive equations describing the thermodynamic state of the mixture of solid pyroclasts, volcanic gas, and air (see Suzuki et al. [4] for details). We assume that no particles separate from the eruption clouds when their size is sufficiently small (< 4 mm). In order to reproduce the general feature of turbulent mixing that the efficiency of entrainment is independent of the

Reynolds number [8], the grid sizes must be sufficiently smaller than the characteristic length scale of the flow. In the case of eruption columns, the characteristic length scale is represented by the radial scale of the flow at each height; it ranges from the vent diameter, D_0, near the vent up to several tens of kilometers far from the vent. Suzuki et al. [4] showed that grid sizes smaller than $D_0/10$ correctly reproduce turbulent mixing near the vent. In order to effectively simulate the turbulent mixing with high spatial resolutions both near the vent and far from it, we have developed a 3-D code in which the domain is descretized on a non-uniform grid. The grid size is set to be sufficiently smaller than $D_0/10$ (typically $D_0/16$) near the vent, and to increase at a constant rate (1.01 for the vertical coordinate and 1.02 for the horizontal coordinate) with the distance from the vent up to $D_0/2$, such that the grid size is small enough to resolve the turbulent flow far from the vent.

From the 3-D simulations, we can directly determine local k using the following relationship [cf. 9, 10]:

$$k = Q_{in}/2\pi\rho_a LW \,, \quad (1)$$

where Q_{in} is the mass inflow of ambient air, ρ_a is the atmospheric density, and L is the radius of the eruption column at each height. The value of LW is given by

$$LW = \left(\int_0^\infty w^2\, rdr\right)^{1/2} \,, \quad (2)$$

where w is the time-averaged vertical velocity, and r is the radial coordinate. In addition to the value of LW, the value of Q_{in} is required to estimate local k from Eq. (1).

The value of Q_{in} is estimated from the flow field that is averaged in time. The time-averaged flow field in and around the eruption column is divided into two regions with respect to flow directions. Inside the eruption column, the flow is predominantly vertical and the time-averaged radial velocity, u, is negligible. Outside the eruption column, on the other hand, the flow is approximately radial, and the time-averaged vertical velocity, w, is nearly zero. Using these features in the time-averaged flow field, we can calculate the radial mass inflow around the eruption column:

$$Q_{in,1} = 2\pi\rho_a ru \,. \quad (3)$$

Because of the mass conservation of the radial mass inflow, $2\pi\rho_a ru$ remains constant regardless of r away from the column edge. This constant value outside the eruption column represents Q_{in}.

The value of Q_{in} can also be estimated from a method that utilizes the vertical mass flux inside the column, M as

$$Q_{in,2} = dM/dz \,, \quad (4)$$

where

$$M = \int_0^\infty 2\pi\rho wrdr. \quad (5)$$

When the flow of the eruption column reaches a steady-state, $Q_{in,2}$ must be equal to $Q_{in,1}$. In Section 3, we present the variation of local k based on $Q_{in,1}$; local k based on $Q_{in,2}$ is used to confirm the steadiness of flow as well as the consistency of the two methods.

Table 1 Input Parameters of the Simulations

Simulation	L_0(m)	m_0 (kg s^{-1})	w_0 (m s^{-1})	T_0 (K)
Run 1	45	4.0 x 10^6	180	1053
Run 2	40	3.2 x 10^6	181	1053
Run 3	57	6.3 x 10^6	179	1053

3. Results

We carried out three simulations for explosive eruptions from a circular vent into a stationary atmosphere under the tropical condition (Table 1). An initial mass fraction of volcanic gas of n_{g0}=0.06 is assumed. The source conditions are set to be steady and pressure-balanced with a vent velocity equal to the sound velocity of the ejected material.

Our primary concern is how the efficiency of entrainment in eruption columns deviates from those for pure jets or plumes ejected from point sources. For this purpose, it is important to set vent radii sufficiently smaller than the length scale at

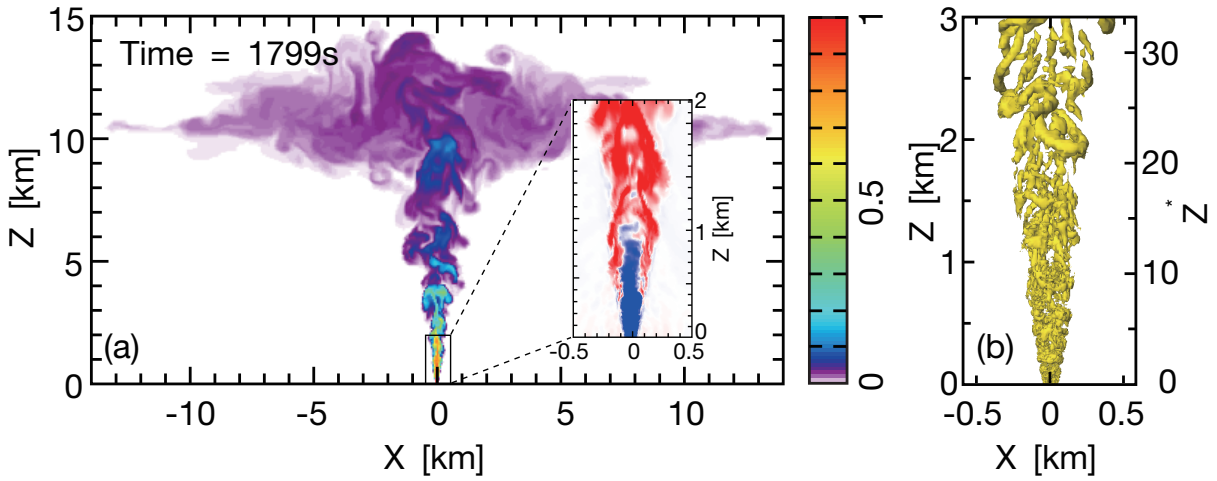

Fig. 1 Numerical results of an eruption column at 1799 s from the beginning of eruption in run 1. (a) Cross-sectional distributions of the mass fraction of magma and (inset) the density difference relative to the stratified atmospheric density at the same vertical position, $-\Delta\rho/\rho_a = 1-\rho/\rho_a$, in $x-z$ space. (b) Isosurface of swirling strength (0.2).

which the initial upward momentum is lost (2-3 km) in the simulations. When the vent radius is greater than a few hundred meters, the eruption cloud loses its momentum before turbulent mixing fully develops from the edge to the core of the flow; as a result, the heavy unmixed core forms a radially suspended flow whose global feature is qualitatively different from those of typical turbulent jets or plumes [4, 11]. In order to avoid additional effects caused by such qualitative differences in flow patterns, we set vent radii to be less than 60 m in this study; the corresponding magma discharge rates range from 10^6 to 10^7 kg s^{-1} (see Table 1).

Our simulations have successfully reproduced the time evolutions of eruption columns (Fig. 1). The eruption cloud is ejected from the vent as a turbulent jet with a large density (3.47 kg m^{-3}) relative to the atmospheric density (1.16 kg m^{-3}). As the turbulent jet entrains ambient air, the eruption column rises as a buoyant plume. The radius of the eruption column linearly increases with height. After the eruption column reaches a maximum height, an umbrella cloud spreads radially, while the eruption column is stably sustained above the vent (Fig. 1a for run 1).

The eruption cloud entrains ambient air through unsteady flow due to turbulence in and around the column (inset in Fig. 1a). Near the vent, the entrainment is driven by shear between the cloud and air at the edge of the column; as a result, a concentric structure consisting of an inner flow and an outer shear layer develops. The outer shear layer has a lower density than that of air owing to expansion of entrained air. On the other hand, the inner flow, which is not mixed with ambient air, remains denser than air. The inner flow is eroded by the outer shear layer and disappears at a certain level (at a height of ~1 km for run 1). As the eruption column further ascends, the flow becomes highly unstable and undergoes a meandering instability.

Fig. 2a shows time-averaged distributions of the vertical velocity between 500 and 1799 s for run 1. The radial profile of the vertical velocity is set to be a top-hat shape as a boundary condition at the vent. The velocity profile near the vent (z=0 – 2 km) is subjected to an intense flow development from a top-hat to a Gaussian shape. Above 2 km, the velocity profile is approximated by a Gaussian shape.

From the profiles of w and $2\pi\rho_a ru$ (Fig. 2), we can identify the two distinct flow regions: the inside and outside of the eruption column. Outside the eruption column ($r>2\sigma$ in Fig. 2), the value of $2\pi\rho_a ru$ remains constant. In this study, we estimate $Q_{in,1}$ from the spatial average of $2\pi\rho_a ru$ in the range of $2\sigma < r < 3\sigma$ at each height for two directions. We confirmed that the value of $Q_{in,1}$ is consistent with $Q_{in,2}$ at each height (figures not shown).

Substituting $Q_{in,1}$ into Eq. (1), we obtain the value of local k as a function of height (Fig. 3). The vertical profiles of k for different mass discharge rates ranging from 10^6 to 10^7 kg s^{-1} show a universal feature when the downstream distance from the vent is normalized by D_0. The value of k decreases with height from 0.07 to 0.05 just above the vent. The region of $3 < z^* < 15$ is characterized by a small value of k~0.05. The value of k increases with height in the range of $15 < z^* < 30$, and approaches a constant value of 0.10 – 0.15.

The value of k decreases again with height above the level where the umbrella cloud begins to develop ($z^* > 60$); however, we do not consider this tendency further, because our estimation based on Eqs. (3) or (4) is no longer applicable for the region where an outward radial flow due to gravity current becomes predominant.

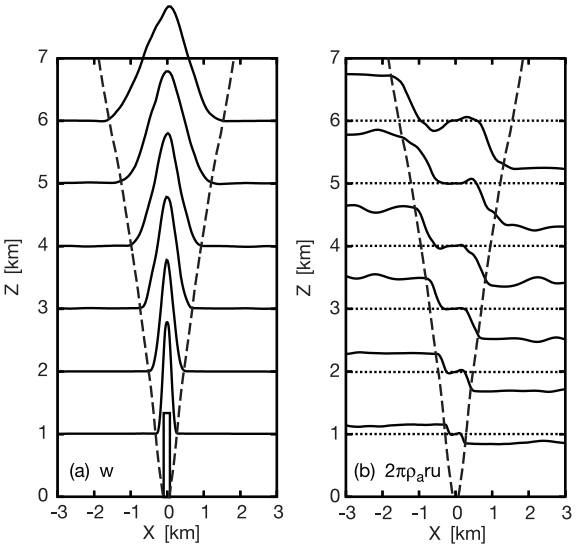

Fig. 2 Time-averaged radial profiles of (a) the vertical velocity and (b) the radial mass flux ($2\pi\rho_a ru$) at different heights in run 1. Dashed curves in the figures are the position of $r=2\sigma$. Note that the value of $2\pi\rho_a ru$ does not depend on x outside of the plume.

4. Discussion

The direct measurements of local k show that k is equal to that for pure jets (~0.07) just above the vent and approaches that for pure plumes (0.10 – 0.15) far from the vent. These features are consistent with the fact that eruption columns are driven by the initial momentum near the vent and by buoyancy far from the vent. Between these two regions we identify a transitional zone with a small local k (~0.05). The presence of this transitional zone is one of the most distinct characteristics of entrainment in eruption columns.

Figure 1b illustrates the change of vortical structures with height. Turbulence in the region where the concentric structure with a dense inner flow and an outer shear layer develops (corresponding to $z^* < 15$) consists of relatively small isotropic vortices, whereas turbulence far from the vent is characterized by large elongated hairpin structures. The position of the change in the vortical structure roughly coincides with the position where the value of k begins to increase. This suggests that the change in vortical structure accompanying the density change controls the efficiency of entrainment including the small local k

in the transitional zone.

In conclusion, we have revealed that the efficiency of entrainment significantly varies with height. This variation is considered to control column heights and the condition of column collapse. To gain a further understanding of the entrainment mechanism, 3-D numerical simulations will be a powerful tool for exploring the role of vortical structures in turbulent mixing.

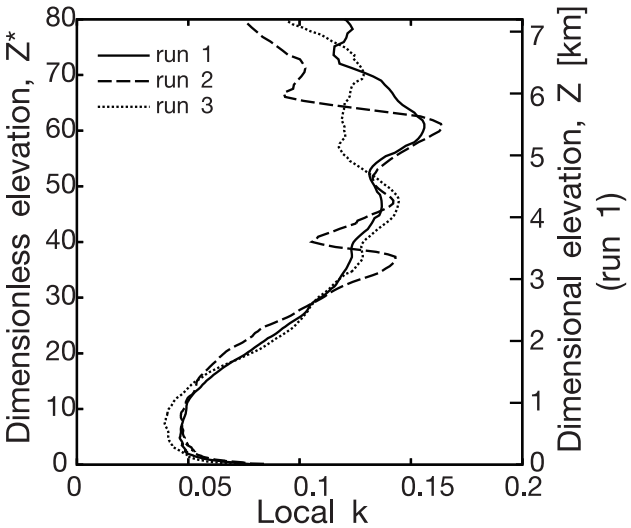

Fig. 3 The vertical distribution of the efficiency of entrainment (local *k*) for runs 1, 2, and 3.

Acknowledgement

A part of this work was performed under the inter-university cooperative research program of Earthquake Research Institute, University of Tokyo.

References

[1] B. R. Morton, G. I. Taylor, and J. S. Turner, "Turbulent gravitational convection from maintained and instantaneous source", Proc. R. Soc. London, Ser. A, 234, 1-23, 1956.

[2] A. W. Woods, "The dynamics of explosive volcanic eruptions", Rev. Geophys., 33(4), 495-530, 1995.

[3] E. Kaminski, S. Tait, and G. Carazzo, "Turbulent entrainment in jets with arbitrary buoyancy", J. Fluid Mech., 526, 361-376, 2005.

[4] Y. J. Suzuki, T. Koyaguchi, M. Ogawa, and I. Hachisu, "A numerical study of turbulent mixing in eruption clouds using a three-dimensional fluid dynamics model", J. Geophys. Res., 110, B08201, 2005.

[5] Y. J. Suzuki, and T. Koyaguchi, "A three-dimensional numerical simulation of spreading umbrella clouds", J. Geophys. Res., 114, B03209, 2009.

[6] P. N. Papanicolaou, and E. J. List, "Investigations of round vertical turbulent buoyant jets", J. Fluid Mech., 195, 341-391, 1988.

[7] H. Wang, and A. W. –K. Law, "Second-order integral model for a round turbulent buoyant jet", J. Fluid Mech., 459, 397-428, 2000.

[8] P. E. Dimotakis, "The mixing transition in turbulent flows", J. Fluid Mech., 409, 69-98, 2000.

[9] M. V. Pham, F. Plourde, and S. D. Kim, "Large-eddy simulation of a pure thermal plume under rotating conditions", Phys. Fluids, 18, 015101, 2006.

[10] F. Plourde, M. V. Pham, S. D. Kim, and S. Balachandar, "Direct numerical simulations of a rapidly expanding thermal plume: Structure and entrainment interaction", J. Fluid Mech., 604, 99-123, 2008.

[11] A. Neri, and F. Dobran, "Influence of erupton parameters on the thermofluid dynamics of collapsing volcanic columns", J. Geophys. Res., 99(B6), 11,833-11,857, 1994.

爆発的火山噴火における噴煙内部の乱流混合効率

プロジェクト責任者
小屋口剛博　　東京大学　地震研究所
著者
鈴木雄治郎　　海洋研究開発機構　地球内部ダイナミクス領域
小屋口剛博　　東京大学　地震研究所

本プロジェクトでは、大規模数値シミュレーションを用いた固体地球と地球表層・大気にまたがる火山現象の理解と計算結果の防災への応用を目指している。本年は特に、火山噴煙内における乱流混合について研究を進めた。

爆発的火山噴火では、火山ガスと火山灰からなる噴出物が周囲の大気を混合し、取り込んだ大気を火山灰の熱で膨張させることで浮力を得て上昇する。この噴煙の最高到達高度、水平方向の広がり、火砕流の発生条件は、大気の取り込み量を決める乱流混合に支配される。一般に、乱流ジェットや乱流プルームでは、平均上昇速度に対する周囲流体の取り込み速度の割合を混合効率の指標とし、エントレインメント係数（k）と呼ぶ。密度成層のない流体中での乱流ジェットや乱流プルームは自己相似性を持ち、k は一定値をとることが知られている（乱流ジェット：0.07、乱流プルーム：0.10 – 0.15）。大気が成層構造を持ち、非線形な密度変化をする噴煙の場合では、その混合効率は場所によって変化し、k の値が一定とはならない可能性がある。そこで、数値シミュレーション結果に基づき、半径方向の大気流入量を直接測定することで取り込み速度と平均上昇速度の比から k の値を高さの関数として求めた。数値コードには一般座標系を適用し、火口付近と噴煙全体の流れのスケールや乱流混合を同時に再現できるようにした。

計算の結果、k の値が高さによって大きく変化し、噴煙内で乱流混合の効率が変化することが分かった。火口の直上での k の値は 0.07 と密度成層のない流体中での乱流ジェットの値に近く、噴煙柱上部での k の値は 0.10 – 0.15 と乱流プルームの値に漸近する。火口直上から噴煙柱上部の間には遷移領域が存在し、k の値は 0.05 と非常に小さな値を取ることが新たに確認された。これらの k の値の高さ変化は、火口からの距離を火口直径で規格化したときに火口での噴火条件（噴出率）に依存せず、噴煙に共通する性質であることが分かった。

3 次元シミュレーション結果から密度構造や渦構造（swirling strength）の 3 次元可視化を行い、乱流混合効率と渦構造の関係を調べた。噴煙柱下部では、流れの中心軸付近に大気とまだ混合していない高濃度噴煙の芯が残り、そこでの乱流は比較的小さく等方的な渦で構成されている。一方、噴煙柱上部では、中心軸付近まで大気との混合が進み、そこでの乱流は大きくて引き伸ばされたヘアピン構造で特徴付けられる。これらの渦構造が変化する高さは、k の値が 0.05 から 0.10-0.15 に変化する高さとほぼ一致することが分かった。

キーワード：火山噴煙, 擬似ガスモデル, 乱流混合, 火山災害